Interfacial Tension during Mass Transfer of CO_2 into Water in a Water-Saturated CO_2 Atmosphere at 298 K and 6.6 MPa

Andreas Hebach,* Guilhem Martin, Andrea Kögel, and Nicolaus Dahmen

Institute for Technical Chemistry-CPV − Forschungszentrum Karlsruhe GmbH, P.O. Box 3640, 76021 Karlsruhe, Germany

Fast measurements of the interfacial tension (IFT) of the water + carbon dioxide system at 298 K and 6.6 MPa were conducted by a modified pendant drop method to investigate the influence of nonequilibrium composition during the mass transfer of CO_2 into the water drops. An apparent decrease in interfacial tension could be attributed to the use of equilibrium densities in their determination. Using the density gradient as it occurs during mass transfer by the measurable volume increase due to CO_2 uptake, we found that the interfacial tension is constant all of the time. For this reason, it is vital to take the density gradient into account if the time-dependent interfacial tension is measured. This gradient can also be used to determine densities in nonequilibrium compositions. The uncertainty of the density determination for the unsaturated water density in the water + carbon dioxide system is strikingly low, lower than 1%.

1. Introduction

Interfacial tension (IFT) is an important, and often unknown, property that is relevant to many technical processes. If data are available, then they have been obtained either under equilibrium conditions assuming a static measuring procedure or by dynamic methods continuously creating a new surface. In an earlier paper, we could show that under equilibrium conditions the IFT data is still subject to changes due to drop aging.[1] For reliable data, one has to consider what we called a quasi-static measuring method of the pendant drop method. We stated that an initial decrease of IFT can be found because of fast processes to attain equilibrium in the water + carbon dioxide system, where a small but non-negligible mutual miscibility in the range of interest exists. This aspect is further elaborated on in this paper because processes ocurring during and immediately after drop formation are important for a variety of technical processes. For example, in liquid−liquid extraction as carried out in countercurrent columns, a considerable portion of the mass transfer occurs during the first seconds after drop formation. In this context, the question arises as to if and to which extent mass transfer across an interface affects IFT. Especially in the case, when the equilibrium composition strongly depends on temperature and pressure, as is the case in systems containing highly compressed phases, a substantial dependence of IFT on composition is possible. Consequently, the question is raised as to if a dynamic change of IFT with changing composition while approaching equilibrium can be expected.

In the present paper, for a fixed temperature and pressure of 298 K and 6.6 MPa, the change in IFT of a water drop pending in water-saturated liquid CO_2 as a function of time was investigated. Fast algorithms for sessile drop analysis were taken from Busoni et al.[2] and adopted for high-pressure pendant drop measurements.

* Corresponding author. E-mail: andreas.hebach@itc-cpv.fzk.de. Fax: +49 7247 82-2244.

2. Experimental Section

In this paper, γ' represents the measured interfacial tension for a fixed density difference of 1000 kg m^{-3}. The IFT as obtained by the saturated densities is denoted by γ_s, and the one derived from the unsaturated densities is denoted by $\gamma_u(t)$. The measured data are listed in Table 1.

Apparatus and Calculation. The apparatus used is described in detail in a previous publication.[1] Briefly, the system consists of a high-pressure viewing cell with a capillary. Water is fed directly to this capillary, and the high-pressure circuit is filled with CO_2. To saturate the CO_2 phase, we filled parts of the viewing cell with water and recirculated the CO_2. The whole system is installed in a climatic chamber, which allows a temperature adjustment within ±0.2 K. The pressure stability is ±0.02 MPa. The IFT is determined by a computer-controlled drop shape analysis with an experimental uncertainty of <2%. In this paper, we report on findings that were obtained with a newly written analysis program. The basic algorithms used were provided by Busoni et al.[2] according to the terms of the GPL license. Their program has been written in C and Fortran running on a Linux distribution RedHat 7.x and 8.0 to evaluate sessile drops. We modified the code. It now runs on a MS Windows 2000 system as usual graphic user interface and is suited to the measurement of pendant drops. The live video image is displayed permanently on the screen along with a results window. From the temperature and pressure data, the corresponding densities of the drop and of the surrounding phase are determined by reference equations.[3,4] All data are stored in an ASCII file for later analysis. The modified software is able to follow dynamic processes such as mixing phenomena with a time resolution of 350 ms.

Basically, for the software a standard density difference of 1000 kg m^{-3} was set, yielding a standardized IFT value, called γ'. Later, the actual γ values were calculated by multiplying γ' by the real density difference (eq 1).

$$\gamma = \frac{\gamma'(\rho_{H_2O} - \rho_{CO_2})}{1000} \tag{1}$$

10.1021/je049773j CCC: $30.25
Published on Web 01/04/2005

Table 1. Measured Data

t / ms	V / mm^3	$\rho_{H_2O}(t)$ / $kg\ m^{-3}$	γ' / $mN\ m^2\ kg^{-1}$	γ_s / $mN\ m^{-1}$	γ_u / $mN\ m^{-1}$	t / ms	V / mm^3	$\rho_{H_2O}(t)$ / $kg\ m^{-3}$	γ' / $mN\ m^2\ kg^{-1}$	γ_s / $mN\ m^{-1}$	γ_u / $mN\ m^{-1}$
218	40.15	999.8	120.0	35.5	33.9	34 547	41.01	1006.9	117.0	34.6	33.8
1062	40.14	999.8	119.7	35.4	33.8	34 968	41.01	1006.9	117.0	34.6	33.8
1484	40.17	1000.0	119.4	35.4	33.7	35 390	41.02	1007.0	116.9	34.6	33.8
1890	40.17	1000.0	119.4	35.4	33.7	35 812	41.03	1007.0	116.9	34.6	33.9
3109	40.25	1000.6	119.4	35.4	33.8	36 234	41.04	1007.1	116.9	34.6	33.9
3531	40.27	1000.8	119.4	35.4	33.8	36 640	41.05	1007.2	116.9	34.6	33.9
3953	40.29	1001.0	119.3	35.3	33.8	37 047	41.05	1007.2	116.9	34.6	33.9
5937	40.34	1001.4	119.1	35.3	33.8	37 468	41.06	1007.3	116.8	34.6	33.9
6781	40.37	1001.6	119.0	35.2	33.8	37 890	41.07	1007.3	116.8	34.6	33.9
7187	40.40	1001.8	119.0	35.2	33.8	38 297	41.08	1007.5	116.8	34.6	33.9
7593	40.41	1002.0	118.9	35.2	33.8	38 718	41.08	1007.5	116.8	34.6	33.9
8015	40.42	1002.0	118.9	35.2	33.8	39 140	41.08	1007.4	116.7	34.6	33.8
8437	40.43	1002.1	118.8	35.2	33.8	39 547	41.08	1007.5	116.7	34.6	33.8
8859	40.44	1002.2	118.8	35.2	33.8	39 953	41.09	1007.5	116.7	34.6	33.8
9265	40.45	1002.3	118.7	35.2	33.8	40 375	41.10	1007.6	116.7	34.5	33.8
9687	40.46	1002.4	118.7	35.1	33.8	40 781	41.09	1007.6	116.6	34.5	33.8
10 093	40.48	1002.5	118.6	35.1	33.8	41 187	41.11	1007.6	116.6	34.5	33.8
10 500	40.49	1002.6	118.6	35.1	33.8	41 593	41.11	1007.7	116.6	34.5	33.8
10 922	40.49	1002.6	118.5	35.1	33.8	42 000	41.11	1007.7	116.6	34.5	33.8
11 343	40.50	1002.7	118.5	35.1	33.8	42 422	41.12	1007.8	116.6	34.5	33.8
11 765	40.52	1002.8	118.4	35.1	33.8	44 218	41.16	1008.1	116.6	34.5	33.9
12 187	40.52	1002.9	118.3	35.0	33.8	44 625	41.16	1008.1	116.5	34.5	33.8
12 609	40.53	1003.0	118.3	35.0	33.8	45 031	41.17	1008.2	116.5	34.5	33.9
13 031	40.54	1003.0	118.3	35.0	33.8	45 453	41.18	1008.3	116.5	34.5	33.9
13 453	40.55	1003.1	118.2	35.0	33.8	45 859	41.19	1008.3	116.5	34.5	33.9
13 875	40.57	1003.3	118.2	35.0	33.8	46 265	41.19	1008.4	116.5	34.5	33.9
14 281	40.58	1003.3	118.2	35.0	33.8	46 672	41.20	1008.4	116.5	34.5	33.9
14 703	40.59	1003.4	118.1	35.0	33.8	47 078	41.20	1008.4	116.4	34.5	33.9
15 125	40.60	1003.5	118.1	35.0	33.8	47 500	41.21	1008.5	116.4	34.5	33.9
15 531	40.62	1003.6	118.1	35.0	33.8	47 906	41.21	1008.5	116.4	34.5	33.9
15 953	40.63	1003.7	118.1	35.0	33.8	48 312	41.21	1008.5	116.4	34.5	33.9
16 375	40.64	1003.8	118.1	35.0	33.8	48 718	41.22	1008.6	116.4	34.4	33.9
16 797	40.65	1003.9	118.0	35.0	33.8	49 125	41.22	1008.6	116.4	34.4	33.9
17 218	40.67	1004.1	118.0	34.9	33.8	49 531	41.22	1008.6	116.3	34.4	33.8
17 640	40.67	1004.1	118.0	34.9	33.8	49 937	41.22	1008.6	116.3	34.4	33.8
18 062	40.68	1004.2	117.9	34.9	33.8	50 359	41.23	1008.7	116.3	34.4	33.8
18 484	40.70	1004.3	117.9	34.9	33.8	50 765	41.23	1008.7	116.3	34.4	33.8
18 906	40.70	1004.3	117.9	34.9	33.8	51 172	41.24	1008.7	116.3	34.4	33.8
19 328	40.70	1004.4	117.8	34.9	33.8	51 578	41.24	1008.8	116.3	34.4	33.8
19 750	40.72	1004.5	117.8	34.9	33.8	51 984	41.25	1008.8	116.3	34.4	33.9
20 172	40.72	1004.5	117.8	35.0	33.9	52 390	41.26	1008.9	116.3	34.4	33.9
21 984	40.75	1004.8	117.6	34.8	33.8	52 797	41.26	1008.9	116.2	34.4	33.9
22 390	40.76	1004.8	117.6	34.8	33.8	53 203	41.27	1009.0	116.2	34.4	33.9
22 812	40.78	1004.9	117.6	34.8	33.8	53 609	41.27	1009.0	116.2	34.4	33.9
23 234	40.78	1005.0	117.5	34.8	33.8	54 015	41.28	1009.1	116.2	34.4	33.9
23 656	40.79	1005.1	117.5	34.8	33.8	54 437	41.29	1009.1	116.2	34.4	33.9
24 078	40.80	1005.1	117.5	34.8	33.8	54 843	41.29	1009.2	116.2	34.4	33.9
24 922	40.83	1005.4	117.5	34.8	33.8	55 250	41.30	1009.2	116.2	34.4	33.9
25 343	40.83	1005.4	117.4	34.8	33.8	55 656	41.30	1009.3	116.2	34.4	33.9
25 765	40.84	1005.5	117.4	34.8	33.8	56 062	41.30	1009.3	116.2	34.4	33.9
26 593	40.87	1005.7	117.4	34.8	33.8	56 468	41.31	1009.3	116.2	34.4	33.9
27 015	40.88	1005.8	117.4	34.7	33.8	56 875	41.31	1009.4	116.2	34.4	33.9
27 437	40.88	1005.8	117.3	34.7	33.8	57 281	41.32	1009.4	116.1	34.4	33.9
27 843	40.90	1006.0	117.5	34.8	33.9	57 687	41.32	1009.4	116.1	34.4	33.9
28 265	40.90	1005.9	117.3	34.7	33.8	58 093	41.32	1009.4	116.1	34.4	33.9
28 672	40.90	1006.0	117.2	34.7	33.8	58 515	41.33	1009.5	116.1	34.4	33.9
29 093	40.91	1006.1	117.2	34.7	33.8	58 922	41.33	1009.5	116.1	34.4	33.9
29 515	40.91	1006.0	117.2	34.7	33.8	59 328	41.33	1009.5	116.0	34.3	33.9
29 922	40.92	1006.1	117.1	34.7	33.8	59 734	41.33	1009.5	116.0	34.3	33.9
30 343	40.91	1006.1	117.1	34.7	33.8	60 140	41.34	1009.6	116.0	34.3	33.9
30 765	40.93	1006.2	117.1	34.7	33.8	60 547	41.34	1009.6	116.0	34.3	33.9
31 172	40.94	1006.3	117.1	34.7	33.8	60 953	41.35	1009.6	116.0	34.3	33.9
31 593	40.95	1006.3	117.1	34.7	33.8	61 375	41.35	1009.7	116.0	34.3	33.9
32 015	40.95	1006.4	117.0	34.7	33.8	61 781	41.36	1009.7	116.0	34.3	33.9
32 437	40.96	1006.5	117.0	34.7	33.8	62 187	41.36	1009.7	116.0	34.3	33.9
32 859	40.97	1006.5	117.0	34.6	33.8	62 593	41.36	1009.8	116.0	34.3	33.9
33 281	40.98	1006.6	117.0	34.6	33.8	63 000	41.37	1009.8	116.0	34.3	33.9
33 703	40.99	1006.7	117.0	34.6	33.8	63 406	41.38	1009.9	116.0	34.3	33.9

Table 1 (Continued)

t (ms)	V (mm^3)	$\rho_{H_2O}(t)$ ($kg\ m^{-3}$)	γ' ($mN\ m^2\ kg^{-1}$)	γ_s ($mN\ m^{-1}$)	γ_u ($mN\ m^{-1}$)	t (ms)	V (mm^3)	$\rho_{H_2O}(t)$ ($kg\ m^{-3}$)	γ' ($mN\ m^2\ kg^{-1}$)	γ_s ($mN\ m^{-1}$)	γ_u ($mN\ m^{-1}$)
63 812	41.38	1009.9	116.0	34.3	33.9	94 437	41.58	1011.5	115.5	34.2	33.9
64 218	41.38	1009.9	116.0	34.3	33.9	94 843	41.58	1011.6	115.5	34.2	33.9
66 047	41.40	1010.1	115.9	34.3	33.9	95 250	41.59	1011.6	115.5	34.2	33.9
66 468	41.41	1010.2	115.9	34.3	33.9	95 656	41.59	1011.6	115.5	34.2	33.9
66 890	41.41	1010.2	115.9	34.3	33.9	96 062	41.59	1011.6	115.4	34.2	33.9
67 312	41.41	1010.1	115.9	34.3	33.9	96 484	41.59	1011.6	115.5	34.2	33.9
67 718	41.41	1010.2	115.9	34.3	33.9	96 890	41.59	1011.7	115.4	34.1	33.9
68 125	41.42	1010.2	115.9	34.3	33.9	97 297	41.59	1011.6	115.4	34.1	33.9
68 531	41.42	1010.2	115.9	34.3	33.9	97 703	41.60	1011.7	115.5	34.2	33.9
68 937	41.42	1010.2	115.8	34.3	33.9	98 109	41.60	1011.7	115.4	34.1	33.9
69 343	41.42	1010.2	115.8	34.3	33.9	98 531	41.60	1011.7	115.4	34.1	33.9
69 750	41.42	1010.2	115.8	34.3	33.9	98 937	41.60	1011.7	115.4	34.1	33.9
70 156	41.43	1010.3	115.8	34.3	33.9	99 343	41.60	1011.7	115.4	34.1	33.9
70 562	41.43	1010.3	115.8	34.3	33.9	99 750	41.60	1011.7	115.4	34.1	33.9
70 968	41.43	1010.3	115.8	34.3	33.9	100 156	41.61	1011.8	115.4	34.1	33.9
71 390	41.44	1010.4	115.8	34.3	33.9	100 562	41.61	1011.8	115.4	34.1	33.9
71 797	41.44	1010.4	115.8	34.3	33.9	100 968	41.61	1011.8	115.4	34.1	33.9
72 203	41.45	1010.5	115.8	34.3	33.9	101 375	41.62	1011.8	115.4	34.1	33.9
72 609	41.45	1010.5	115.8	34.3	33.9	101 781	41.61	1011.8	115.4	34.1	33.9
73 015	41.45	1010.5	115.8	34.3	33.9	102 187	41.62	1011.8	115.4	34.1	33.9
73 437	41.46	1010.5	115.8	34.3	33.9	102 593	41.62	1011.8	115.4	34.1	33.9
73 843	41.46	1010.5	115.8	34.3	33.9	103 000	41.62	1011.8	115.4	34.1	33.9
74 250	41.46	1010.6	115.8	34.2	33.9	103 406	41.62	1011.9	115.4	34.1	33.9
74 656	41.48	1010.7	115.8	34.3	33.9	103 812	41.63	1011.9	115.4	34.1	33.9
75 062	41.47	1010.6	115.7	34.2	33.9	104 218	41.62	1011.9	115.4	34.1	33.9
75 484	41.47	1010.7	115.7	34.2	33.9	104 625	41.62	1011.9	115.4	34.1	33.9
75 890	41.48	1010.7	115.7	34.2	33.9	105 031	41.62	1011.9	115.4	34.1	33.9
76 297	41.49	1010.8	115.8	34.2	33.9	105 453	41.63	1012.0	115.4	34.1	33.9
76 703	41.48	1010.7	115.7	34.2	33.9	105 875	41.63	1011.9	115.4	34.1	33.9
77 109	41.49	1010.8	115.7	34.2	33.9	106 281	41.63	1011.9	115.4	34.1	33.9
77 515	41.49	1010.8	115.7	34.2	33.9	106 687	41.63	1012.0	115.4	34.1	33.9
77 922	41.49	1010.8	115.7	34.2	33.9	107 093	41.63	1012.0	115.4	34.1	33.9
78 328	41.49	1010.8	115.7	34.2	33.9	107 515	41.63	1012.0	115.4	34.1	33.9
78 734	41.49	1010.8	115.7	34.2	33.9	107 922	41.63	1012.0	115.3	34.1	33.9
79 140	41.49	1010.8	115.7	34.2	33.9	109 734	41.64	1012.0	115.3	34.1	33.9
79 547	41.50	1010.9	115.7	34.2	33.9	110 140	41.64	1012.1	115.3	34.1	33.9
79 953	41.50	1010.9	115.7	34.2	33.9	110 547	41.64	1012.1	115.3	34.1	33.9
80 359	41.50	1010.9	115.6	34.2	33.9	110 953	41.64	1012.1	115.3	34.1	33.9
80 765	41.50	1010.9	115.6	34.2	33.9	111 375	41.64	1012.0	115.3	34.1	33.9
81 172	41.51	1010.9	115.6	34.2	33.9	111 781	41.64	1012.0	115.3	34.1	33.9
81 578	41.51	1011.0	115.6	34.2	33.9	112 187	41.65	1012.1	115.3	34.1	33.9
81 984	41.51	1011.0	115.6	34.2	33.9	112 593	41.65	1012.1	115.3	34.1	33.9
82 406	41.51	1011.0	115.6	34.2	33.9	113 000	41.64	1012.1	115.3	34.1	33.9
82 812	41.52	1011.0	115.6	34.2	33.9	113 406	41.65	1012.1	115.3	34.1	33.9
83 218	41.53	1011.1	115.6	34.2	33.9	114 015	41.65	1012.1	115.3	34.1	33.9
83 625	41.52	1011.1	115.6	34.2	33.9	114 422	41.66	1012.2	115.3	34.1	33.9
84 031	41.53	1011.1	115.6	34.2	33.9	114 828	41.65	1012.2	115.3	34.1	33.9
84 453	41.53	1011.1	115.6	34.2	33.9	115 234	41.66	1012.2	115.3	34.1	33.9
84 859	41.52	1011.1	115.6	34.2	33.9	115 640	41.66	1012.2	115.3	34.1	33.9
85 265	41.53	1011.1	115.6	34.2	33.9	116 047	41.66	1012.2	115.3	34.1	33.9
85 672	41.54	1011.2	115.6	34.2	33.9	116 453	41.66	1012.2	115.3	34.1	33.9
86 078	41.54	1011.2	115.6	34.2	33.9	116 859	41.66	1012.2	115.2	34.1	33.9
87 906	41.56	1011.4	115.6	34.2	33.9	117 265	41.66	1012.2	115.3	34.1	33.9
88 312	41.55	1011.3	115.6	34.2	33.9	117 672	41.67	1012.3	115.3	34.1	33.9
88 718	41.55	1011.3	115.6	34.2	33.9	118 078	41.66	1012.2	115.2	34.1	33.9
89 125	41.55	1011.3	115.5	34.2	33.9	118 484	41.66	1012.2	115.3	34.1	33.9
89 531	41.56	1011.3	115.5	34.2	33.9	118 890	41.67	1012.3	115.3	34.1	33.9
89 937	41.55	1011.3	115.5	34.2	33.9	119 297	41.67	1012.3	115.2	34.1	33.9
90 343	41.56	1011.4	115.5	34.2	33.9	119 703	41.67	1012.3	115.3	34.1	33.9
90 750	41.56	1011.4	115.5	34.2	33.9	120 109	41.68	1012.4	115.3	34.1	34.0
91 172	41.56	1011.4	115.5	34.2	33.9	120 515	41.67	1012.3	115.3	34.1	33.9
91 578	41.57	1011.4	115.5	34.2	33.9	120 922	41.67	1012.3	115.2	34.1	33.9
91 984	41.57	1011.4	115.5	34.2	33.9	121 328	41.67	1012.3	115.2	34.1	33.9
92 406	41.57	1011.5	115.5	34.2	33.9	121 734	41.68	1012.3	115.2	34.1	33.9
92 812	41.57	1011.5	115.5	34.2	33.9	122 140	41.67	1012.3	115.2	34.1	33.9
93 218	41.58	1011.5	115.5	34.2	33.9	122 547	41.67	1012.3	115.2	34.1	33.9
93 625	41.58	1011.5	115.5	34.2	33.9	122 953	41.67	1012.3	115.2	34.1	33.9
94 031	41.58	1011.5	115.5	34.2	33.9	123 359	41.68	1012.4	115.2	34.1	33.9

Table 1 (Continued)

t / ms	V / mm^3	$\rho_{H_2O}(t)$ / kg m^{-3}	γ' / mN m^2 kg^{-1}	γ_s / mN m^{-1}	γ_u / mN m^{-1}	t / ms	V / mm^3	$\rho_{H_2O}(t)$ / kg m^{-3}	γ' / mN m^2 kg^{-1}	γ_s / mN m^{-1}	γ_u / mN m^{-1}
123 765	41.68	1012.4	115.2	34.1	33.9	154 187	41.74	1012.9	115.0	34.1	34.0
124 172	41.68	1012.4	115.2	34.1	33.9	154 593	41.74	1012.8	115.0	34.1	34.0
124 578	41.68	1012.4	115.2	34.1	33.9	155 000	41.74	1012.9	115.0	34.1	34.0
124 984	41.68	1012.4	115.2	34.1	33.9	155 406	41.74	1012.9	115.1	34.1	34.0
125 390	41.69	1012.5	115.2	34.1	34.0	155 812	41.75	1012.9	115.1	34.1	34.0
125 797	41.68	1012.4	115.2	34.1	33.9	156 218	41.74	1012.9	115.1	34.1	34.0
126 203	41.68	1012.4	115.2	34.1	33.9	156 625	41.75	1012.9	115.1	34.1	34.0
126 609	41.69	1012.4	115.2	34.1	33.9	157 031	41.75	1012.9	115.0	34.1	34.0
127 015	41.68	1012.4	115.2	34.1	33.9	157 437	41.75	1012.9	115.1	34.1	34.0
127 422	41.69	1012.4	115.2	34.1	33.9	157 843	41.75	1013.0	115.1	34.1	34.0
127 828	41.69	1012.4	115.2	34.1	33.9	158 250	41.75	1012.9	115.1	34.1	34.0
128 234	41.69	1012.5	115.2	34.1	33.9	158 656	41.75	1012.9	115.1	34.1	34.0
128 640	41.69	1012.5	115.2	34.1	33.9	159 062	41.75	1013.0	115.1	34.1	34.0
129 047	41.69	1012.4	115.2	34.1	33.9	159 468	41.76	1013.0	115.1	34.1	34.0
129 453	41.69	1012.5	115.2	34.1	33.9	159 875	41.75	1012.9	115.0	34.1	34.0
129 859	41.69	1012.5	115.2	34.1	33.9	160 281	41.75	1013.0	115.0	34.1	34.0
131 656	41.70	1012.5	115.1	34.1	33.9	160 687	41.76	1013.0	115.0	34.1	34.0
132 062	41.70	1012.5	115.2	34.1	34.0	161 093	41.76	1013.0	115.1	34.1	34.0
132 468	41.70	1012.6	115.2	34.1	34.0	161 500	41.76	1013.0	115.1	34.1	34.0
132 875	41.70	1012.5	115.2	34.1	34.0	161 906	41.76	1013.0	115.0	34.1	34.0
133 281	41.70	1012.5	115.2	34.1	34.0	162 312	41.76	1013.0	115.1	34.1	34.0
133 687	41.70	1012.6	115.2	34.1	34.0	162 718	41.76	1013.0	115.0	34.0	34.0
134 093	41.70	1012.6	115.1	34.1	33.9	163 125	41.76	1013.0	115.0	34.0	34.0
134 500	41.71	1012.6	115.2	34.1	34.0	163 531	41.76	1013.0	115.0	34.0	34.0
134 906	41.71	1012.6	115.2	34.1	34.0	163 937	41.76	1013.0	115.0	34.1	34.0
135 312	41.71	1012.6	115.1	34.1	33.9	164 343	41.77	1013.1	115.1	34.1	34.0
135 718	41.71	1012.6	115.2	34.1	34.0	164 750	41.76	1013.0	115.0	34.0	34.0
136 125	41.71	1012.6	115.1	34.1	34.0	165 156	41.76	1013.0	115.0	34.1	34.0
136 531	41.71	1012.6	115.1	34.1	34.0	165 562	41.76	1013.0	115.0	34.0	34.0
136 937	41.71	1012.6	115.1	34.1	34.0	165 968	41.76	1013.0	115.0	34.1	34.0
137 343	41.72	1012.7	115.2	34.1	34.0	166 375	41.77	1013.1	115.1	34.1	34.0
137 750	41.71	1012.6	115.1	34.1	34.0	166 781	41.76	1013.0	115.0	34.1	34.0
138 156	41.71	1012.6	115.1	34.1	34.0	167 187	41.76	1013.0	115.0	34.1	34.0
138 562	41.72	1012.7	115.1	34.1	34.0	167 593	41.76	1013.0	115.0	34.0	34.0
138 968	41.73	1012.7	115.1	34.1	34.0	168 000	41.76	1013.0	115.0	34.0	34.0
139 375	41.72	1012.7	115.1	34.1	34.0	168 406	41.76	1013.0	115.0	34.0	34.0
139 781	41.72	1012.7	115.1	34.1	34.0	168 812	41.77	1013.1	115.0	34.0	34.0
140 187	41.72	1012.7	115.1	34.1	34.0	169 218	41.77	1013.1	115.0	34.0	34.0
140 593	41.72	1012.7	115.1	34.1	34.0	169 625	41.76	1013.0	115.0	34.0	34.0
141 000	41.72	1012.7	115.1	34.1	33.9	170 031	41.76	1013.1	115.0	34.0	34.0
141 406	41.72	1012.7	115.1	34.1	34.0	170 437	41.77	1013.1	115.0	34.1	34.0
141 812	41.72	1012.7	115.1	34.1	34.0	170 843	41.77	1013.1	115.0	34.0	34.0
142 218	41.73	1012.8	115.1	34.1	34.0	17 1250	41.77	1013.1	115.0	34.0	34.0
142 625	41.73	1012.8	115.1	34.1	34.0	171 656	41.77	1013.1	115.0	34.0	34.0
143 031	41.73	1012.8	115.1	34.1	34.0	172 062	41.76	1013.1	115.0	34.0	34.0
143 437	41.73	1012.8	115.1	34.1	34.0	172 468	41.77	1013.1	115.0	34.0	34.0
143 843	41.72	1012.7	115.1	34.1	34.0	172 875	41.77	1013.1	115.0	34.0	34.0
144 250	41.73	1012.8	115.1	34.1	34.0	173 281	41.77	1013.1	115.0	34.0	34.0
144 656	41.73	1012.8	115.1	34.1	34.0	175 078	41.77	1013.1	115.0	34.0	34.0
145 062	41.73	1012.8	115.1	34.1	34.0	175 484	41.77	1013.1	115.0	34.0	34.0
145 468	41.73	1012.8	115.1	34.1	34.0	175 890	41.77	1013.1	115.0	34.0	34.0
145 875	41.73	1012.8	115.1	34.1	34.0	176 297	41.77	1013.1	115.0	34.0	34.0
146 281	41.74	1012.9	115.1	34.1	34.0	176 703	41.77	1013.1	115.0	34.0	34.0
146 687	41.73	1012.8	115.1	34.1	34.0	177 109	41.77	1013.1	115.0	34.0	34.0
147 093	41.74	1012.8	115.1	34.1	34.0	177 531	41.78	1013.2	115.0	34.0	34.0
147 500	41.73	1012.8	115.0	34.0	33.9	177 937	41.77	1013.1	115.0	34.0	34.0
147 906	41.73	1012.8	115.1	34.1	34.0	178 343	41.78	1013.2	115.0	34.0	34.0
148 312	41.73	1012.8	115.1	34.1	34.0	178 750	41.77	1013.1	115.0	34.0	34.0
148 718	41.74	1012.8	115.1	34.1	34.0	179 156	41.77	1013.1	115.0	34.0	34.0
149 125	41.74	1012.8	115.1	34.1	34.0	179 562	41.77	1013.1	115.0	34.0	34.0
149 531	41.74	1012.8	115.1	34.0	34.0	179 968	41.77	1013.1	114.9	34.0	34.0
149 937	41.73	1012.8	115.1	34.0	33.9	180 375	41.77	1013.1	115.0	34.0	34.0
150 359	41.74	1012.8	115.1	34.0	34.0	180 781	41.77	1013.1	115.0	34.0	34.0
150 765	41.74	1012.8	115.0	34.0	34.0	181 187	41.77	1013.1	115.0	34.0	34.0
151 172	41.74	1012.9	115.1	34.1	34.0	181 593	41.77	1013.1	115.0	34.0	34.0
151 578	41.74	1012.8	115.1	34.1	34.0	182 000	41.77	1013.1	115.0	34.0	34.0
153 375	41.74	1012.8	115.0	34.1	34.0	182 406	41.78	1013.2	115.0	34.0	34.0
153 781	41.74	1012.9	115.1	34.1	34.0	182 812	41.78	1013.2	115.0	34.0	34.0

Table 1 (Continued)

t / ms	V / mm^3	$\rho_{H_2O}(t)$ / kg m^{-3}	γ' / mN m^2 kg^{-1}	γ_s / mN m^{-1}	γ_u / mN m^{-1}	t / ms	V / mm^3	$\rho_{H_2O}(t)$ / kg m^{-3}	γ' / mN m^2 kg^{-1}	γ_s / mN m^{-1}	γ_u / mN m^{-1}
183 218	41.77	1013.1	115.0	34.0	34.0	212 672	41.79	1013.3	114.9	34.0	34.0
183 625	41.78	1013.1	115.0	34.0	34.0	213 078	41.79	1013.3	114.9	34.0	34.0
184 031	41.78	1013.2	115.0	34.0	34.0	213 484	41.79	1013.3	114.9	34.0	34.0
184 437	41.78	1013.2	115.0	34.0	34.0	213 890	41.80	1013.3	114.9	34.0	34.0
184 843	41.78	1013.2	115.0	34.0	34.0	214 297	41.79	1013.3	114.9	34.0	34.0
185 250	41.78	1013.2	115.0	34.0	34.0	214 703	41.79	1013.3	114.9	34.0	34.0
185 656	41.78	1013.2	115.0	34.0	34.0	215 109	41.79	1013.3	114.9	34.0	34.0
186 062	41.78	1013.2	115.0	34.0	34.0	215 515	41.80	1013.3	114.9	34.0	34.0
186 468	41.78	1013.2	115.0	34.0	34.0	215 922	41.80	1013.3	114.9	34.0	34.0
186 875	41.78	1013.2	115.0	34.0	34.0	216 328	41.80	1013.3	114.9	34.0	34.0
187 281	41.78	1013.2	114.9	34.0	34.0	216 734	41.80	1013.3	114.9	34.0	34.0
187 687	41.78	1013.2	114.9	34.0	34.0	218 562	41.81	1013.4	114.9	34.0	33.9
188093	41.78	1013.2	115.0	34.0	34.0	218 968	41.81	1013.4	114.9	34.0	34.0
188515	41.78	1013.2	115.0	34.0	34.0	219 375	41.81	1013.4	114.9	34.0	34.0
188 922	41.78	1013.2	115.0	34.0	34.0	219 781	41.81	1013.4	114.9	34.0	34.0
189 328	41.78	1013.2	115.0	34.0	34.0	220 187	41.80	1013.4	114.9	34.0	33.9
189 734	41.78	1013.2	115.0	34.0	34.0	220 593	41.80	1013.3	114.9	34.0	33.9
190 140	41.78	1013.2	115.0	34.0	34.0	221 000	41.80	1013.4	114.9	34.0	33.9
190 547	41.78	1013.2	115.0	34.0	34.0	221 406	41.80	1013.4	114.9	34.0	33.9
190 953	41.78	1013.2	114.9	34.0	34.0	221 812	41.80	1013.4	114.9	34.0	33.9
191 359	41.78	1013.2	115.0	34.0	34.0	222 218	41.80	1013.4	114.9	34.0	33.9
191 765	41.78	1013.2	114.9	34.0	34.0	222 625	41.80	1013.4	114.9	34.0	33.9
192 172	41.78	1013.2	115.0	34.0	34.0	223 031	41.80	1013.4	114.9	34.0	33.9
192 578	41.78	1013.2	115.0	34.0	34.0	223 437	41.80	1013.4	114.9	34.0	33.9
192 984	41.78	1013.2	115.0	34.0	34.0	223 843	41.80	1013.4	114.9	34.0	33.9
193 390	41.78	1013.2	114.9	34.0	34.0	224 250	41.81	1013.4	114.9	34.0	34.0
193 797	41.78	1013.2	114.9	34.0	34.0	224 656	41.80	1013.4	114.9	34.0	33.9
194 203	41.78	1013.2	115.0	34.0	34.0	225 062	41.80	1013.3	114.9	34.0	33.9
194 609	41.78	1013.2	115.0	34.0	34.0	225 468	41.80	1013.4	114.9	34.0	33.9
195 015	41.78	1013.2	114.9	34.0	34.0	225 875	41.80	1013.4	114.9	34.0	33.9
196 812	41.78	1013.2	115.0	34.0	34.0	226 281	41.80	1013.4	114.9	34.0	33.9
197 218	41.79	1013.2	115.0	34.0	34.0	226 687	41.80	1013.4	114.9	34.0	33.9
197 625	41.78	1013.2	114.9	34.0	34.0	227 093	41.80	1013.4	114.9	34.0	33.9
198 031	41.79	1013.2	115.0	34.0	34.0	227 500	41.81	1013.4	114.9	34.0	34.0
198 437	41.80	1013.3	115.0	34.0	34.0	227 906	41.80	1013.4	114.9	34.0	33.9
198 843	41.79	1013.2	115.0	34.0	34.0	228 312	41.80	1013.4	114.9	34.0	33.9
199 250	41.79	1013.2	114.9	34.0	34.0	228 718	41.80	1013.3	114.9	34.0	33.9
199 656	41.79	1013.3	114.9	34.0	34.0	229 125	41.80	1013.4	114.9	34.0	33.9
200 062	41.80	1013.3	115.0	34.0	34.0	229 531	41.80	1013.4	114.9	34.0	33.9
200 484	41.80	1013.3	114.9	34.0	34.0	229 937	41.80	1013.4	114.9	34.0	33.9
200 890	41.80	1013.3	115.0	34.0	34.0	230 343	41.80	1013.3	114.9	34.0	33.9
201 297	41.79	1013.3	115.0	34.0	34.0	230 750	41.80	1013.4	114.9	34.0	33.9
201 703	41.79	1013.2	114.9	34.0	34.0	231 156	41.80	1013.4	114.9	34.0	33.9
202 109	41.79	1013.3	114.9	34.0	34.0	231 562	41.81	1013.4	114.9	34.0	33.9
202 515	41.79	1013.3	114.9	34.0	34.0	231 968	41.80	1013.4	114.9	34.0	33.9
202 922	41.79	1013.3	114.9	34.0	34.0	232 375	41.80	1013.4	114.9	34.0	33.9
203 328	41.79	1013.2	114.9	34.0	34.0	232 781	41.80	1013.4	114.9	34.0	33.9
203 734	41.79	1013.3	114.9	34.0	34.0	233 187	41.81	1013.4	114.9	34.0	34.0
204 140	41.79	1013.3	114.9	34.0	34.0	233 593	41.80	1013.4	114.9	34.0	33.9
204 547	41.79	1013.3	114.9	34.0	34.0	234 000	41.80	1013.3	114.9	34.0	33.9
204 953	41.79	1013.3	114.9	34.0	34.0	234 406	41.81	1013.4	114.9	34.0	33.9
205 359	41.79	1013.3	114.9	34.0	34.0	234 812	41.80	1013.4	114.9	34.0	33.9
205 765	41.79	1013.3	114.9	34.0	34.0	235 218	41.80	1013.4	114.9	34.0	33.9
206 172	41.79	1013.2	114.9	34.0	34.0	235 625	41.80	1013.4	114.9	34.0	33.9
206 578	41.79	1013.3	114.9	34.0	34.0	236 031	41.81	1013.4	114.9	34.0	33.9
206 984	41.79	1013.3	115.0	34.0	34.0	236 453	41.81	1013.4	114.9	34.0	33.9
207 390	41.79	1013.3	114.9	34.0	34.0	236 859	41.81	1013.4	114.9	34.0	33.9
207 797	41.79	1013.3	114.9	34.0	34.0	237 265	41.81	1013.4	114.9	34.0	33.9
208 203	41.79	1013.3	114.9	34.0	34.0	237 672	41.81	1013.5	114.9	34.0	34.0
208 609	41.80	1013.3	114.9	34.0	34.0	238 078	41.81	1013.5	114.9	34.0	33.9
209 015	41.79	1013.3	114.9	34.0	34.0	238 484	41.81	1013.4	114.9	34.0	33.9
209 422	41.79	1013.3	114.9	34.0	34.0	240 281	41.81	1013.4	114.9	34.0	33.9
209 828	41.79	1013.3	114.9	34.0	34.0	240 687	41.82	1013.5	114.9	34.0	34.0
210 234	41.79	1013.3	114.9	34.0	34.0	241 093	41.81	1013.4	114.9	34.0	34.0
210 640	41.79	1013.3	114.9	34.0	34.0	241 500	41.81	1013.4	114.9	34.0	34.0
211 047	41.79	1013.3	114.9	34.0	34.0	241 906	41.81	1013.4	114.9	34.0	33.9
211 453	41.79	1013.3	114.9	34.0	34.0	242 718	41.81	1013.4	114.9	34.0	33.9
212 265	41.79	1013.3	114.9	34.0	34.0	243 125	41.82	1013.5	114.9	34.0	34.0

Table 1 (Continued)

t / ms	V / mm^3	$\rho_{H_2O}(t)$ / kg m^{-3}	γ' / mN m^2 kg^{-1}	γ_s / mN m^{-1}	γ_u / mN m^{-1}	t / ms	V / mm^3	$\rho_{H_2O}(t)$ / kg m^{-3}	γ' / mN m^2 kg^{-1}	γ_s / mN m^{-1}	γ_u / mN m^{-1}
243 531	41.80	1013.4	114.9	34.0	33.9	272 578	41.80	1013.4	114.8	34.0	33.9
243 937	41.81	1013.4	114.9	34.0	34.0	272 984	41.81	1013.4	114.9	34.0	34.0
244 343	41.81	1013.4	114.9	34.0	33.9	273 390	41.79	1013.3	114.8	34.0	33.9
244 750	41.82	1013.5	114.9	34.0	34.0	274 187	41.79	1013.3	114.8	34.0	33.9
245 156	41.81	1013.4	114.8	34.0	33.9	275 000	41.82	1013.5	114.9	34.0	34.0
245 578	41.81	1013.4	114.9	34.0	33.9	275 406	41.82	1013.5	114.8	34.0	34.0
245 984	41.81	1013.4	114.9	34.0	34.0	275 812	41.82	1013.5	114.8	34.0	34.0
246 390	41.81	1013.4	114.9	34.0	34.0	276 625	41.82	1013.5	114.8	34.0	34.0
246 797	41.81	1013.4	114.9	34.0	33.9	277 031	41.82	1013.5	114.8	34.0	34.0
247 203	41.81	1013.4	114.8	34.0	33.9	277 437	41.82	1013.5	114.8	34.0	34.0
247 609	41.81	1013.4	114.9	34.0	34.0	277 843	41.82	1013.5	114.8	34.0	34.0
248 015	41.81	1013.4	114.8	34.0	33.9	278 250	41.83	1013.6	114.9	34.0	34.0
248 422	41.81	1013.4	114.9	34.0	33.9	279 062	41.83	1013.6	114.8	34.0	34.0
248 828	41.81	1013.4	114.9	34.0	34.0	279 468	41.83	1013.6	114.8	34.0	34.0
249 234	41.81	1013.4	114.9	34.0	34.0	279 875	41.83	1013.6	114.8	34.0	34.0
249 640	41.81	1013.4	114.9	34.0	34.0	280 281	41.83	1013.6	114.9	34.0	34.0
250 047	41.81	1013.4	114.9	34.0	33.9	280 687	41.83	1013.6	114.9	34.0	34.0
250 453	41.81	1013.4	114.9	34.0	34.0	281 093	41.83	1013.6	114.8	34.0	34.0
250 859	41.81	1013.4	114.8	34.0	33.9	281 500	41.83	1013.6	114.8	34.0	34.0
251 265	41.81	1013.5	114.9	34.0	34.0	281 906	41.82	1013.6	114.8	34.0	34.0
251 672	41.81	1013.4	114.8	34.0	33.9	284 515	41.83	1013.6	114.8	34.0	34.0
252 078	41.81	1013.5	114.9	34.0	34.0	285 328	41.83	1013.6	114.8	34.0	34.0
252 500	41.81	1013.4	114.9	34.0	33.9	286 953	41.83	1013.6	114.8	34.0	34.0
252 906	41.81	1013.4	114.9	34.0	34.0	287 359	41.83	1013.6	114.8	34.0	34.0
253 312	41.81	1013.4	114.8	34.0	33.9	287 765	41.83	1013.6	114.8	34.0	34.0
253 718	41.81	1013.5	114.9	34.0	34.0	288 578	41.82	1013.6	114.8	34.0	34.0
254 125	41.81	1013.4	114.8	34.0	33.9	288 984	41.83	1013.6	114.8	34.0	34.0
254 531	41.81	1013.4	114.8	34.0	33.9	293 062	41.83	1013.6	114.8	34.0	34.0
254 937	41.81	1013.5	114.8	34.0	33.9	301 609	41.83	1013.6	114.8	34.0	34.0
255 343	41.81	1013.5	114.9	34.0	34.0	309 093	41.83	1013.6	114.8	34.0	34.0
255 750	41.81	1013.5	114.8	34.0	33.9	313 562	41.83	1013.6	114.8	34.0	34.0
256 156	41.81	1013.5	114.9	34.0	34.0	314 781	41.83	1013.6	114.8	34.0	34.0
256 562	41.82	1013.5	114.9	34.0	34.0	317 218	41.83	1013.6	114.8	34.0	34.0
256 968	41.82	1013.5	114.9	34.0	34.0	318 843	41.83	1013.6	114.8	34.0	34.0
257 375	41.81	1013.5	114.9	34.0	34.0	319 656	41.83	1013.6	114.8	34.0	34.0
257 781	41.82	1013.5	114.9	34.0	34.0	320 062	41.83	1013.6	114.8	34.0	34.0
258 187	41.82	1013.5	114.9	34.0	34.0	320 875	41.83	1013.6	114.8	34.0	34.0
258 593	41.81	1013.5	114.9	34.0	33.9	321 281	41.84	1013.7	114.8	34.0	34.0
259 000	41.82	1013.5	114.9	34.0	34.0	322 093	41.83	1013.6	114.8	34.0	34.0
259 406	41.82	1013.5	114.8	34.0	34.0	322 500	41.84	1013.7	114.8	34.0	34.0
259 812	41.82	1013.5	114.9	34.0	34.0	322 906	41.84	1013.7	114.8	34.0	34.0
260 218	41.82	1013.5	114.9	34.0	34.0	323 312	41.83	1013.6	114.8	34.0	34.0
262 015	41.82	1013.5	114.9	34.0	34.0	323 718	41.80	1013.4	114.7	33.9	33.9
262 422	41.82	1013.5	114.9	34.0	34.0	324 125	41.82	1013.5	114.8	34.0	33.9
262 828	41.81	1013.5	114.8	34.0	34.0	324 531	41.79	1013.3	114.7	33.9	33.9
263 234	41.82	1013.5	114.9	34.0	34.0	324 937	41.79	1013.3	114.7	33.9	33.9
263 640	41.82	1013.5	114.8	34.0	34.0	325 343	41.83	1013.6	114.8	34.0	34.0
264 047	41.82	1013.5	114.8	34.0	34.0	327 140	41.82	1013.6	114.8	34.0	33.9
264 453	41.81	1013.5	114.8	34.0	34.0	327 547	41.82	1013.5	114.8	33.9	33.9
264 859	41.81	1013.5	114.9	34.0	34.0	327 953	41.83	1013.6	114.8	34.0	34.0
265 265	41.82	1013.5	114.9	34.0	34.0	328 359	41.82	1013.5	114.8	33.9	33.9
265 672	41.82	1013.5	114.9	34.0	34.0	328 765	41.82	1013.5	114.8	33.9	33.9
266 078	41.82	1013.5	114.9	34.0	34.0	329 172	41.83	1013.6	114.8	34.0	34.0
266 484	41.82	1013.5	114.9	34.0	34.0	329 578	41.82	1013.5	114.8	34.0	33.9
266 890	41.82	1013.5	114.9	34.0	34.0	329 984	41.83	1013.6	114.8	34.0	33.9
267 297	41.81	1013.5	114.8	34.0	34.0	330 390	41.82	1013.5	114.8	34.0	33.9
267 703	41.82	1013.5	114.9	34.0	34.0	330 797	41.82	1013.5	114.8	33.9	33.9
268 109	41.81	1013.5	114.8	34.0	34.0	331 203	41.82	1013.6	114.8	34.0	33.9
268 515	41.81	1013.4	114.9	34.0	34.0	331 609	41.82	1013.5	114.8	34.0	33.9
268 922	41.82	1013.5	114.9	34.0	34.0	332 0 15	41.82	1013.5	114.8	34.0	33.9
269 328	41.82	1013.5	114.9	34.0	34.0	332 422	41.82	1013.5	114.8	33.9	33.9
269 734	41.82	1013.5	114.9	34.0	34.0	332 828	41.83	1013.6	114.8	33.9	33.9
270 140	41.82	1013.5	114.9	34.0	34.0	333 234	41.82	1013.5	114.8	34.0	33.9
270 547	41.82	1013.5	114.8	34.0	34.0	333 640	41.83	1013.6	114.8	34.0	34.0
270 953	41.82	1013.5	114.8	34.0	34.0	334 047	41.83	1013.6	114.8	34.0	33.9
271 359	41.82	1013.5	114.8	34.0	34.0	334 453	41.83	1013.6	114.8	33.9	33.9
271 765	41.81	1013.4	114.8	34.0	34.0	334 859	41.82	1013.5	114.8	34.0	33.9
272 172	41.82	1013.5	114.8	34.0	34.0	335 265	41.82	1013.5	114.8	33.9	33.9

Table 1 (Continued)

t / ms	V / mm^3	$\rho_{H_2O}(t)$ / kg m^{-3}	γ' / mN m^2 kg^{-1}	γ_s / mN m^{-1}	γ_u / mN m^{-1}	t / ms	V / mm^3	$\rho_{H_2O}(t)$ / kg m^{-3}	γ' / mN m^2 kg^{-1}	γ_s / mN m^{-1}	γ_u / mN m^{-1}
335 672	41.82	1013.5	114.8	33.9	33.9	398 406	41.83	1013.6	114.8	33.9	33.9
336 078	41.82	1013.6	114.8	34.0	33.9	398 812	41.82	1013.5	114.8	34.0	33.9
336 484	41.83	1013.6	114.8	34.0	34.0	399 218	41.82	1013.5	114.8	34.0	33.9
336 890	41.82	1013.5	114.8	34.0	33.9	399 625	41.83	1013.6	114.8	34.0	33.9
337 297	41.83	1013.6	114.8	34.0	33.9	400 031	41.82	1013.5	114.8	34.0	33.9
337 703	41.82	1013.5	114.8	34.0	33.9	400 437	41.82	1013.5	114.7	33.9	33.9
338 109	41.83	1013.6	114.8	34.0	33.9	400 843	41.82	1013.5	114.8	33.9	33.9
338 515	41.82	1013.5	114.8	34.0	33.9	401 250	41.83	1013.6	114.8	34.0	33.9
338 922	41.82	1013.5	114.8	33.9	33.9	401 656	41.83	1013.6	114.8	34.0	33.9
339 328	41.83	1013.6	114.8	34.0	33.9	402 062	41.82	1013.5	114.8	33.9	33.9
339 734	41.83	1013.6	114.8	34.0	34.0	402 468	41.82	1013.5	114.8	34.0	33.9
340 140	41.82	1013.5	114.8	33.9	33.9	402 875	41.83	1013.6	114.8	34.0	34.0
340 547	41.83	1013.6	114.8	34.0	33.9	403 281	41.83	1013.6	114.8	34.0	34.0
340 953	41.82	1013.5	114.8	33.9	33.9	403 687	41.83	1013.6	114.7	33.9	33.9
341 359	41.83	1013.6	114.8	34.0	34.0	404 109	41.83	1013.6	114.8	34.0	33.9
341 765	41.84	1013.6	114.8	34.0	34.0	404 515	41.82	1013.5	114.7	33.9	33.9
342 172	41.83	1013.6	114.8	34.0	34.0	404 922	41.82	1013.5	114.7	33.9	33.9
342 578	41.83	1013.6	114.8	34.0	34.0	405 328	41.82	1013.5	114.8	34.0	33.9
342 984	41.83	1013.6	114.8	34.0	34.0	405 734	41.82	1013.5	114.8	33.9	33.9
343 390	41.82	1013.5	114.8	33.9	33.9	406 140	41.82	1013.5	114.8	33.9	33.9
343 797	41.82	1013.5	114.8	34.0	33.9	406 547	41.82	1013.5	114.8	33.9	33.9
344 203	41.80	1013.4	114.8	33.9	33.9	406 953	41.82	1013.5	114.8	34.0	33.9
345 000	41.82	1013.5	114.8	34.0	33.9	407 359	41.82	1013.5	114.8	34.0	33.9
345 828	41.84	1013.7	114.8	34.0	34.0	407 765	41.83	1013.6	114.8	34.0	34.0
346 234	41.83	1013.6	114.8	34.0	34.0	408 172	41.82	1013.5	114.7	33.9	33.9
346 640	41.83	1013.6	114.8	33.9	33.9	408 578	41.83	1013.6	114.8	34.0	33.9
347 047	41.83	1013.6	114.8	34.0	34.0	408 984	41.82	1013.5	114.7	33.9	33.9
349 250	41.83	1013.6	114.8	33.9	33.9	409 390	41.82	1013.5	114.7	33.9	33.9
350 062	41.83	1013.6	114.8	33.9	33.9	409 797	41.83	1013.6	114.8	34.0	33.9
350 890	41.83	1013.6	114.8	33.9	33.9	410 203	41.82	1013.5	114.7	33.9	33.9
353 328	41.83	1013.6	114.8	33.9	33.9	410 609	41.83	1013.6	114.7	33.9	33.9
353 734	41.83	1013.6	114.8	33.9	33.9	411 015	41.83	1013.6	114.8	33.9	33.9
361 453	41.84	1013.7	114.8	33.9	34.0	411 422	41.83	1013.6	114.7	33.9	33.9
362 672	41.83	1013.6	114.8	33.9	33.9	411 828	41.82	1013.5	114.7	33.9	33.9
366 734	41.83	1013.6	114.8	33.9	33.9	412 234	41.82	1013.5	114.7	33.9	33.9
367 140	41.83	1013.6	114.8	33.9	33.9	414 031	41.82	1013.5	114.8	33.9	33.9
367 953	41.84	1013.7	114.8	33.9	33.9	414 875	41.83	1013.6	114.7	33.9	33.9
368 359	41.83	1013.6	114.8	33.9	33.9	416 500	41.80	1013.3	114.7	33.9	33.9
373 422	41.83	1013.6	114.8	34.0	34.0	416 922	41.82	1013.5	114.8	33.9	33.9
376 265	41.84	1013.6	114.8	34.0	34.0	417 328	41.83	1013.6	114.8	33.9	33.9
377 078	41.83	1013.6	114.8	34.0	34.0	417 734	41.82	1013.5	114.8	33.9	33.9
377 890	41.83	1013.6	114.8	34.0	34.0	418 140	41.82	1013.5	114.7	33.9	33.9
378 703	41.83	1013.6	114.8	34.0	34.0	418 547	41.82	1013.5	114.7	33.9	33.9
37 9922	41.83	1013.6	114.8	34.0	34.0	418 953	41.82	1013.5	114.8	33.9	33.9
380 328	41.83	1013.6	114.8	34.0	34.0	419 359	41.82	1013.5	114.7	33.9	33.9
381 968	41.84	1013.6	114.8	34.0	34.0	419 765	41.82	1013.5	114.7	33.9	33.9
382 375	41.84	1013.7	114.8	34.0	34.0	420 172	41.82	1013.5	114.8	33.9	33.9
384 406	41.84	1013.7	114.8	34.0	34.0	420 578	41.82	1013.5	114.7	33.9	33.9
386 031	41.83	1013.6	114.8	34.0	34.0	420 984	41.83	1013.6	114.8	33.9	33.9
386 843	41.83	1013.6	114.8	34.0	34.0	421 390	41.83	1013.6	114.8	33.9	33.9
389 687	41.84	1013.6	114.8	34.0	34.0	421 797	41.83	1013.6	114.7	33.9	33.9
390 093	41.83	1013.6	114.8	34.0	34.0	422 203	41.83	1013.6	114.8	33.9	33.9
390 500	41.82	1013.5	114.8	34.0	34.0	422 609	41.83	1013.6	114.7	33.9	33.9
392 297	41.83	1013.6	114.8	34.0	34.0	423 015	41.82	1013.5	114.7	33.9	33.9
392 703	41.82	1013.5	114.7	33.9	33.9	423 422	41.83	1013.6	114.8	33.9	33.9
393 109	41.82	1013.5	114.7	33.9	33.9	423 828	41.83	1013.6	114.8	33.9	33.9
393 515	41.82	1013.5	114.8	34.0	33.9	424 234	41.83	1013.6	114.7	33.9	33.9
393 922	41.82	1013.5	114.7	33.9	33.9	424 640	41.82	1013.6	114.8	33.9	33.9
394 328	41.82	1013.5	114.8	34.0	33.9	425 047	41.83	1013.6	114.8	33.9	33.9
394 734	41.82	1013.5	114.7	33.9	33.9	425 453	41.83	1013.6	114.8	33.9	33.9
395 140	41.82	1013.5	114.8	34.0	33.9	425 859	41.83	1013.6	114.8	33.9	33.9
395 547	41.82	1013.5	114.8	34.0	33.9	426 265	41.82	1013.5	114.7	33.9	33.9
395 953	41.82	1013.5	114.7	33.9	33.9	426 672	41.83	1013.6	114.7	33.9	33.9
396 375	41.82	1013.5	114.7	33.9	33.9	427 078	41.83	1013.6	114.7	33.9	33.9
396 781	41.82	1013.5	114.8	34.0	33.9	427 484	41.82	1013.5	114.7	33.9	33.9
397 187	41.82	1013.5	114.7	33.9	33.9	427 890	41.83	1013.6	114.8	33.9	33.9
397 593	41.82	1013.5	114.8	34.0	33.9	428 297	41.83	1013.6	114.7	33.9	33.9
398 000	41.82	1013.5	114.7	33.9	33.9	428 703	41.83	1013.6	114.8	33.9	33.9

Table 1 (Continued)

t	V	$\rho_{H_2O}(t)$	γ'	γ_s	γ_u	t	V	$\rho_{H_2O}(t)$	γ'	γ_s	γ_u
ms	mm^3	kg m^{-3}	mN m^2 kg^{-1}	mN m^{-1}	mN m^{-1}	ms	mm^3	kg m^{-3}	mN m^2 kg^{-1}	mN m^{-1}	mN m^{-1}
429 109	41.83	1013.6	114.7	33.9	33.9	431 953	41.82	1013.5	114.8	33.9	33.9
429 515	41.83	1013.6	114.8	33.9	33.9	432 359	41.82	1013.5	114.7	33.9	33.9
429 922	41.83	1013.6	114.8	33.9	33.9	432 765	41.82	1013.5	114.7	33.9	33.9
430 328	41.82	1013.5	114.7	33.9	33.9	433 172	41.82	1013.5	114.8	33.9	33.9
430 734	41.82	1013.5	114.8	33.9	33.9	433 578	41.82	1013.5	114.7	33.9	33.9
431 140	41.83	1013.6	114.7	33.9	33.9	434 000	41.82	1013.5	114.8	33.9	33.9
431 547	41.83	1013.6	114.7	33.9	33.9	435 797	41.83	1013.6	114.8	34.0	34.0

The advantage of this procedure is that the γ' data have a lower uncertainty because there are no density effects within the data. A second advantage is better comparability between different authors because the γ' values do not contain the uncertainties of the density determination.

Validation of the System. The isotherm at 293 K was measured using the quasi-static measuring procedure.[1] For each measured value, a photo of the drop and the boundary lines were saved (Figure 1). The boundary lines are necessary to calculate the IFT value because they determine the parts of the photo including the drop and the capillary. The capillary is used for internal calibration; from the drop shape, the IFT is calculated. These photographs were analyzed by both programs, the previously used commercial software and the new code. The data agree within the experimental error of <2%.

3. Results

To study the initial dynamic processes during and immediately after drop formation in more detail, we exposed a water drop pending to a water-saturated carbon dioxide atmosphere at 298 K and 6.63 MPa. The resulting volume increase due to carbon dioxide mass transfer into the drop is displayed in Figure 2. The origin of the time scale is the starting time of the measurements after drop formation by stopping the water feed. This drop formation itself took approximately 1 s. The time constant for the volume increase is 14.9 ms^{-1}. After 6 min, the system attaines equilibrium. Koegel et al.[5] found similar values, but they missed the first 30 s and their time resolution was in the range of several seconds.

Figure 3 depicts the corresponding γ_s (thick line) and γ_u (thin line) interfacial tension values. The pronounced decrease in γ_s is obtained using the saturated equilibrium density of the water and the carbon dioxide phase at the given conditions of temperature and pressure. In this case, IFT starts at 35.6 mN m^{-1} and decreases asymptotically with a similar time constant of 15.9 ms^{-1} as for the volume change. This trend in the IFT is generally attributed to fast processes of the drop aging process.[6] Usually, diffusion processes, chemical reactions, reorientation of the water structure, and convections are assumed to amount to this decrease.

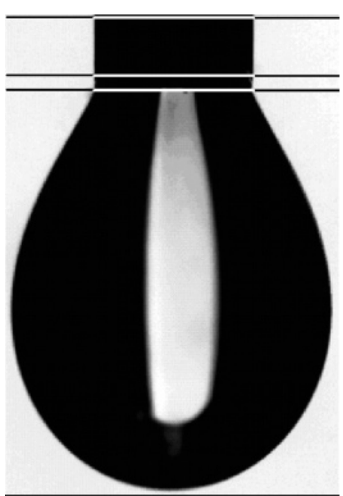

Figure 1. Image of a pending drop. The bars indicate the capillary and drop area.

4. Discussion

We correlated the change in volume—the uptake of CO_2—of the water drop linearly with a change in the drops density (eq 2). At the beginning, the drop consists of pure water, having the density of pure water (999.9 kg m^{-3}) under the measuring conditions.[3] After equilibration took place, the density of the drop is (1013.6 ± 1.0) kg m^{-3} as measured at equilibrium conditions.[4] As the drop changes its volume from 40.16 μL to (41.83 ± 0.01) μL, the linear gradient is 8.2 kg μL^{-1} m^{-3}. The correlation for the water

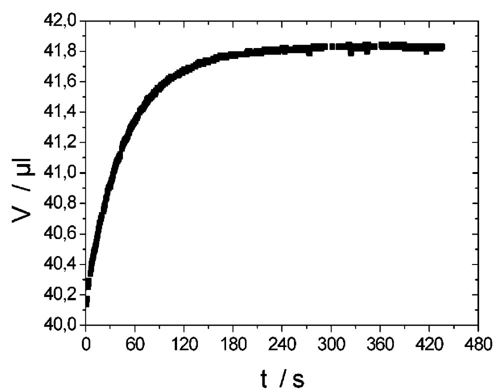

Figure 2. Increase of the drop volume vs time due to CO_2 uptake.

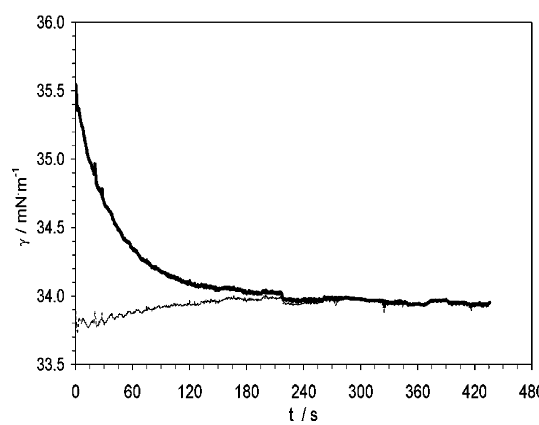

Figure 3. Decrease of γ_s (–) and γ_u (–) vs time.

density ($\rho_{H_2O}(t)$) is shown in eq 2. In this equation, $V(t)$ is the volume of the actual water drop in microliters.

$$\rho_{H_2O}(t) = 8.2 \text{ kg } \mu\text{L}^{-1} \text{ m}^{-3}(V(t) - 40.16 \text{ } \mu\text{L}) + 999.9 \text{ kg m}^{-3} \quad (2)$$

The density of the corresponding water-saturated CO_2 phase is (717.5 ± 0.7) kg m^{-3}. The uncertainty of the density difference is ±0.6%.

Taking the gradient for the water density into consideration, we calculated γ_u. The result is also shown in Figure 3 as a dashed line. In contrast to γ_s, the IFT stays constant. The formation of the interface is much faster than the measuring time. Consequently, before the first measuring point is recorded, the interface is already established. The decay in γ_s as it is shown in Figure 3 is due to an incorrect assumption, namely, that the change in the drop density from the pure water to the mixed-phase density is negligible. This is not true, and considering this, the interfacial tension does not change within the experimental uncertainty.

However, $\gamma'(t)$ can be used to determine the nonequilibrium density of water. Because the IFT can be regarded as constant (see discussion above), the decrease in the $\gamma'(t)$ data can be used to evaluate the correct density difference and hence the water density during mass transfer. Again we use a linear dependency: The starting $\gamma'(t)$ is 120.0 mN m^{-1}, and the actual equilibrium value is 114.8 mN m^{-1}. The gradient for the density is −2.6 kg m^{-2} mN^{-1}. With eq 3, the density of water in the process of saturation can be calculated.

$$\rho_{H_2O}(t) = -2.6 \text{ kg m}^{-2} \text{ mN}^{-1}(\gamma'(t) - 120.0 \text{ mN m}^{-1}) + 999.9 \text{ kg m}^{-3} \quad (3)$$

$\gamma'(t)$ is the interfacial tension value actually determined by the software. Figure 4 displays the match between the water-phase densities. The dashed line is calculated using the drop volume, and the solid line is calculated using the $\gamma'(t)$ values. The deviation between the two curves is less than 1%, lower than the measuring accuracy.

5. Conclusions

In this paper, we report new findings concerning the state of the interface in the process of mass transfer. The interface is established in a much faster time regime than is possible for the measuring. The mass transfer of CO_2 into the water phase and hence the increase in volume and weight of the water drop are still going on when the interface is fully completed. One conclusion is that the IFT of water + CO_2 is constant during mass transfer if the nonequilibrium density of water is taken into account. Because there are significant changes in the water phase in this system and still there is no influence on the interface, this finding might be of a general state. The calculation and modeling of mass-transfer systems becomes simpler, having a constant IFT in certain limits.

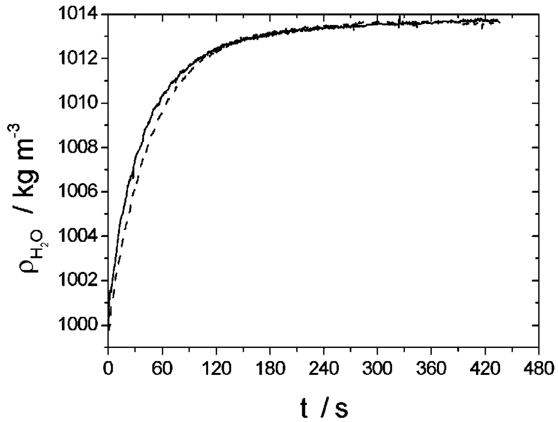

Figure 4. Comparison of the two different methods used to calculate $\rho_{H_2O}(t)$: −, calculated using eq 3; - - -, calculated using eq 2.

From the observed trend in the γ_s slope in Figure 3, the nonequilibrium density of water is calculated. These data coincide with the determined data having an uncertainty of 1%. Therefore, the pendant drop method may be a propper way to determine nonequilibrium density data of phases. This should help to model phase-transition systems more accurate.

Literature Cited

(1) Hebach, A.; Oberhof, A.; Dahmen, N.; Kögel, A.; Ederer, H.; Dinjus, E. Interfacial Tension at Elevated Pressures—Measurements and Correlations in the Water + Carbon Dioxide System. *J. Chem. Eng. Data* **2002**, *47*, 1540−1546.

(2) Busoni, L.; Carla, M.; Lanzi, L. Algorithms for fast axis-symmetric drop shape analysis measurements by a charge coupled device video camera and simulation procedure for test and evaluation. *Rev. Sci. Instrum.* **2001**, *72*, 2784−2791.

(3) Span, R.; Wagner, W. A New Equation of State for Carbon Dioxide Covering the Fluid Region from the Triple-Point Temperature to 1100 K at Pressures up to 800 MPa. *J. Phys. Chem. Ref. Data* **1996**, *25*, 1509−1596.

(4) Hebach, A.; Oberhof, A.; Dahmen, N. *J. Chem. Eng. Data*, accepted for publication.

(5) Kögel, A.; Dahman, N.; Ederer, H. *J. Supercrit. Fluids* **2004**, *29*, 237−249.

(6) Harrison, K. L.; Johnston K. P.; da Rocha, S. R. P. *Langmuir* **1999**, *15*, 419−428.

Received for review June 17, 2004. Accepted November 9, 2004.

JE049773J